

Single dopants in semiconductors

Paul M. Koenraad¹ and Michael E. Flatté²

The sensitive dependence of a semiconductor's electronic, optical and magnetic properties on dopants has provided an extensive range of tunable phenomena to explore and apply to devices. Recently it has become possible to move past the tunable properties of an ensemble of dopants to identify the effects of a solitary dopant on commercial device performance as well as locally on the fundamental properties of a semiconductor. New applications that require the discrete character of a single dopant, such as single-spin devices in the area of quantum information or single-dopant transistors, demand a further focus on the properties of a specific dopant. This article describes the huge advances in the past decade towards observing, controllably creating and manipulating single dopants, as well as their application in novel devices which allow opening the new field of solotronics (solitary dopant optoelectronics).

Early on in semiconductor research, the ubiquity of unintentional dopants meant that reproducible results were rare; as late as 1931, physicist Wolfgang Pauli opined in a letter¹ to Rudolph Peierls that “one shouldn't work on semiconductors, that is a filthy mess; who knows whether any semiconductors exist.” Eight decades later, the purity of germanium is better than 1 part in 10^{11} , permitting almost nine orders of magnitude variability in doping concentration. Silicon purity is similar. Yet even with this current exquisite control, the dopants usually still play a supporting role in current devices, by modifying the chemical potential of a material. At these levels of purity, each unintentional dopant is on average more than a micrometre away from any other unintentional dopant. Thus devices on the nano-scale can be expected to have absolutely no unintentional dopants, and if the doping is carefully controlled a device can be constructed with one and only one dopant — a solitary dopant optoelectronic, or solotronic, device. And, as atoms are the building blocks of matter, a solotronic device is where the miniaturization of semiconductor devices reaches the limits set by the discrete nature of matter.

Although the properties of individual dopants determine some aspects of a doped device (such the dependence of carrier freeze-out on the dopant binding energy), the first effect of individual dopant dynamics on devices was through electronic noise. About 30 years ago one of the main sources of Lorentz noise in metal-oxide-semiconductor field-effect transistor (MOSFET) devices was traced to the trapping and detrapping of charge carriers at impurity centres close to the conduction channel. Owing to the high purity of the semiconductor materials and the increasingly small device sizes, discrete impurities started to show up in most device transport properties. Random telegraph noise from an individual impurity was first observed at low temperatures in MOSFETs² and quantum point contact structures³ and later at room temperature in bipolar transistors⁴. Such developments imply that individual impurities might ultimately dominate the device characteristics of future MOSFET transistors⁵. The potential fluctuations from individual impurities in a MOSFET transistor are shown in Fig. 1a. Controlled positioning of these impurities can improve threshold voltage reproducibility for MOSFETs, as shown in Fig. 1b–e (ref. 6). The International Technology Roadmap for Semiconductors (ITRS) specifically discusses the need for accurate three-dimensional (3D) dopant incorporation, profiling and modelling.

The detection of the discrete properties of solitary dopants in individual devices motivated new device designs that required this

behaviour. About 10 years ago it was realized that single impurities could be used to physically realize the ‘qubits’ of quantum computation, with a single phosphorus dopant's nuclear spin⁷, or a single dopant's bound electron spin⁸ or charge⁹. Single dopants are suggested not only as qubits for quantum computing but also as non-classical light sources in quantum information science for quantum key distribution systems, quantum repeaters, quantum lithography, multivalent logic and local sensing. Single impurities have already shown their importance for non-classical light sources through the demonstration of single-photon emission from nitrogen-vacancy (NV) centres in diamond¹⁰, isoelectronic tellurium impurity centres in ZnSe (ref. 11) and N pairs in GaP (ref. 12) as well as triggered single-photon emission in the case of N-acceptors in ZnSe (ref. 13) and NV centres in diamond¹⁴.

The above examples may be viewed as the initial demonstrations and model device designs on the path to a fully fledged solotronic technology, which requires considerable additional fundamental study and device application. The desirable features of solitary dopants, such as the reproducible quantized properties of a specific dopant, make them ideal objects for further scientific study and robust applications. However, a reliance on the properties of a solitary dopant generates new challenges: device behaviour depends on the local environment (strain, electric, magnetic and optical fields) and the dopant position within the device. Scientific study of single-atom behaviour is most advanced in single-atom and single-ion electromagnetic traps in vacuum; study of the solitary dopant in a solid also takes advantage of a natural form of trapping, as the solitary impurity is held in place by the electromagnetic fields of the host solid around it, but on a length scale orders of magnitude smaller.

Why is our focus on the solitary dopant in a semiconductor, rather than a metal or insulator? To reduce the electronic interaction of the single dopant with the host, and preserve some of the discrete character of the dopant, the host should not be a metal; the overlap of a host metal's electronic states and impurity states is too large for a single impurity to dominate the properties. However, a host insulator is also less than optimal, for to enable the application of external electric fields and couple the single dopant to transport, the host should be a semiconductor. Thus the exploration and manipulation of a single dopant in a semiconducting host should be the focus of solotronic research, and holds promise for device applications as diverse as scalable sources for quantized emission,

¹COBRA Inter-University Research Institute, Department of Applied Physics, Eindhoven University of Technology, PO Box 513, 5600 MB Eindhoven, The Netherlands. ²Department of Physics and Astronomy, University of Iowa, 203 VAN, Iowa City, Iowa 52242, USA. *e-mail: p.m.koenraad@tue.nl; michael_flatte@mailaps.org

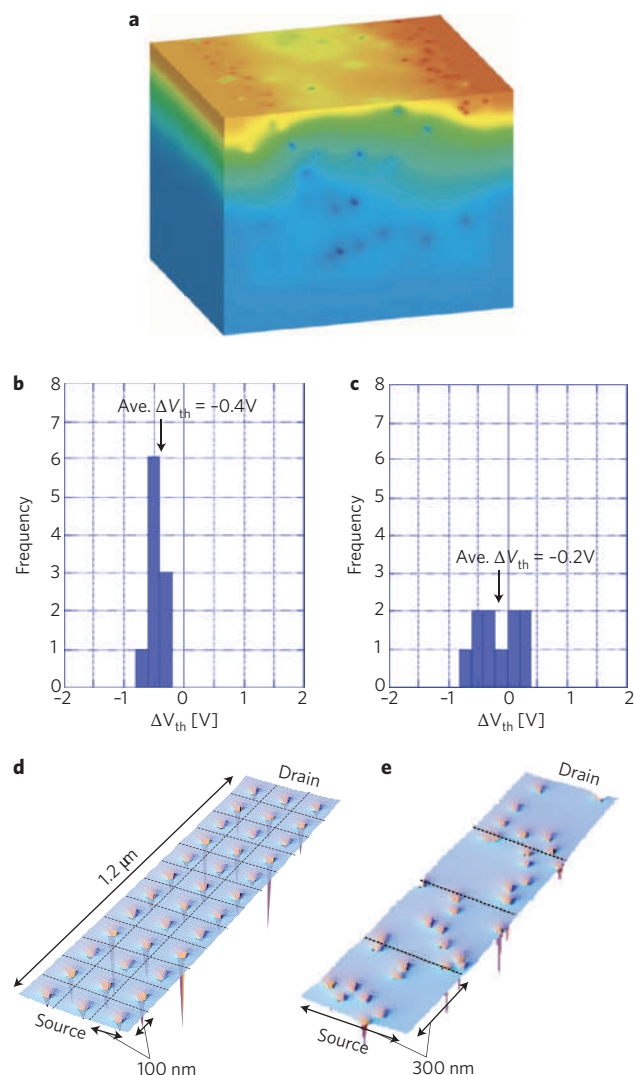


Figure 1 | Impurities in a MOSFET device. **a**, Simulation of the potential distribution in a 50-nm MOSFET device showing the potential fluctuations due to discrete impurities in the conduction channel. **b,c**, Histograms of the measured threshold voltage, V_{th} , in devices with an ordered (**b**) or random (**c**) dopant distribution. **d,e**, Calculated potential distribution in the channel region of a MOSFET with an ordered (**d**) or random (**e**) dopant distribution. Reprinted with permission from: **a**, ref. 5, © 2003 IEEE; **b-e**, ref. 6, © 2005 NPG.

qubits for quantum computation and elements in multivalent logic. Recent scientific developments have brought these options within reach, through experimental advances in scanning probe microscopy, confocal microscopy and single-impurity implantation. These new techniques are able to address, manipulate and even arrange individual impurities. We thus have reached a point where one can start to unravel the interaction of a single impurity with its environment, pioneer the construction of single-impurity devices and explore fundamental quantum-mechanical processes on individually addressable impurities.

Observing single impurities

The first electronic observation of a single impurity in a semiconductor material was made in a MOSFET device cooled to low temperature². A single bistable impurity close to the conduction channel was responsible for the observed random telegraph noise. The observation of random telegraph noise due to single impurities in nanostructured devices is now rather common³, but it remains a challenge

to obtain detailed information about the responsible impurity itself. One exception is the use of noise in a conduction channel to measure the spin state of a single impurity⁸. A spin-to-charge transformation can occur when the impurity, by virtue of the Pauli principle, can only bind a second electron with opposite spin. Recently this tactic was applied to monitor the spin resonance of a single paramagnetic impurity at the Si/SiO₂ interface¹⁵.

Single impurities also manifested their presence in tunnelling. In a double-barrier resonant-tunnelling (DBRT) diode with a micrometre-sized diameter, features in the I - V curves could be related to the presence of a single Si donor in the DBRT well¹⁶. Although DBRT structures enabled the determination of the spin-splitting of an individual Si doping atom located in a GaAs quantum well¹⁷ as well as located in an AlAs barrier¹⁸, and an estimate of the extension of the wavefunction of the impurity state¹⁹, their use is often hampered by the uncontrolled incorporation and unknown chemical nature of the impurity state. Other tunnelling approaches have used a single impurity to scan the density-of-states (DOS) spectrum of a two-dimensional electron gas²⁰ or shown the presence of a single impurity in industrial-type nano-MOSFETs^{21,22}.

Optical identifications of an individual semiconductor impurity followed after tunnelling identification¹⁶, by analysing the electroluminescence of a doped large-area DBRT structure and relating sharp lines to the presence of independent acceptors in the DBRT's well²³. The application of standard high-resolution optical spectroscopy on a GaAs sample with a low density of N-pairs allowed for the first luminescence study of individual isoelectronic N-pairs²⁴. An improved optical assessment of individual impurities, by optical excitation and detection, could be obtained by confocal microscopy in combination with solid immersion lenses that reduce the spot size to about 250 nm in the visible range of the spectrum. This approach allowed the observation of single NV centres in diamond²⁵. A length scale of 250 nm is still large compared with the typical distance between impurities, but new approaches, such as stimulated emission depletion microscopy, show a superior resolution, better than 10 nm for an impurity in diamond²⁶. For more common optical analysis techniques, the impurities have to be spectroscopically singled out from the background, and their concentration must be very low. For NV centres in diamond, which can have concentrations of the order of 10^9 cm⁻³ or even lower depending on the growth conditions, this methodology works very well. Owing to their low density, their spectroscopic isolation from other defects, and their favourable spin properties (for example long spin coherence time at room temperature²⁷), NV centres have become the model system to explore fundamental quantum-mechanical processes on individually addressable impurities²⁸⁻³¹ (see Fig. 2b). Other interesting systems that have been explored as non-classical light sources are N-acceptors in ZnSe (ref. 13), Te isoelectronic centres in ZnSe (ref. 11) and N-N isoelectronic pairs in GaP (ref. 12; Fig. 2a). Single impurities can also be spectroscopically isolated from the other (similar) impurities by trapping small numbers of them, or just one, in a nanostructure with a smaller bandgap than the environment, as is the case for Mn acceptors in a GaAs quantum well³² or for Mn in an InAs or CdTe quantum dot^{33,34}. Optical spin probing³³ and manipulation³⁵ of a single Mn impurity have been shown in Mn-doped CdTe quantum dots.

To assess the magnetic properties of a single impurity, a resonating magnetic cantilever can in principle be used, as has been done successfully to detect single spins on cobalt atoms in glass³⁶. However, local electron spin resonance (ESR) using a scanning probe tip provides a more attractive approach to probe and manipulate a single spin. Precession of a single spin on a partly oxidized silicon (111)- 7×7 surface was reported two decades ago³⁷. More recently, a magnetic-field-dependent ESR signal has been obtained from a single molecule³⁸, and atomically resolved ESR information can currently be obtained on a silicon 7×7 surface³⁹. This opens

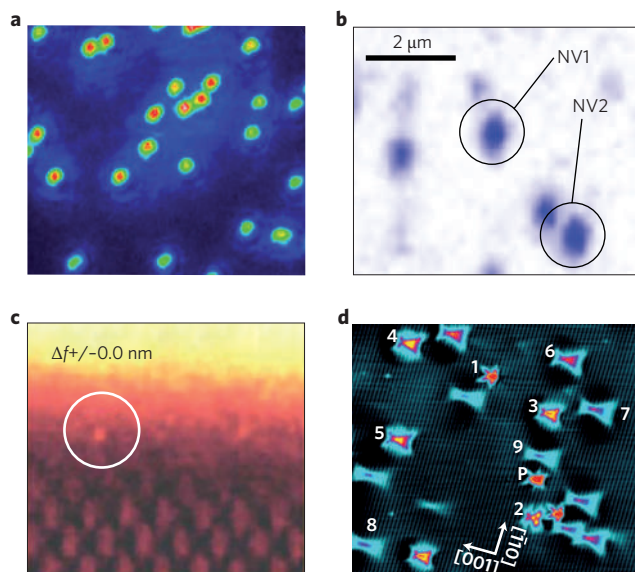


Figure 2 | Imaging of single impurities. Examples of individual impurities in a semiconductor material as observed by several techniques. Observation of **a**, N-N pairs in GaP; **b**, NV centres in diamond by scanning confocal microscopy; **c**, a single Hf atom at the Si-SiO interface by scanning transmission electron microscopy; and **d**, Mn acceptors in GaAs by cross-section STM. The numbers indicate the depth in atomic layers of the Mn layer below the (110) cleavage surface, and p indicates a Mn atom coupled to an adsorbate. Reprinted with permission from: **a**, ref. 12, © 2007 JSAP; **b**, ref. 29, © 2008 APS; **c**, ref. 41, © 2005 AIP; **d**, ref. 92, © 2010 APS.

the route to applying the scanning probe ESR technique to single impurities. The spin information it provides might solve one of the most important outstanding problems for conventional scanning tunnelling microscopy: how to determine the chemical nature of the impurity under the scanning tip.

Observing the spatial location of single impurities in a semiconductor material has been a longstanding challenge for transmission electron microscopy. This was only recently resolved after the development of annular dark-field scanning transmission electron microscopy with a spatial resolution of about 0.2 nm. The first observations of single impurities by this technique were made⁴⁰ on Sb atoms in Si. The same technique in combination with series of through-focus images was finally able to pinpoint the 3D position of individual Hf atoms near a MOSFET interface with an accuracy of 0.5 nm (ref. 41; Fig. 2c). A serious limitation of this technique is the weak scattering of electrons by some impurity species, rendering them undetectable. Promising results in the field of 3D tomography of impurities in semiconductors include the observation of the 3D distribution of (impurity) atoms with a so-called atom probe. This technique removes atoms layer-by-layer by field emission, and uses spatially resolved time-of-flight analysis to determine the original location and atomic mass of the detected atoms⁴². The difficult reconstruction process needed to determine the original position of the detected atoms and impurities in the material and the fact that only a fraction of all atoms can be detected remain serious challenges for this new technique.

In the field of scanning probe microscopy, the positions of impurity atoms were revealed by their impact on the electron propagation as visualized by a scanning gate probe tip⁴³. Later, this scanning gate technique was able to resolve directly the position of individual impurities in a carbon nanotube⁴⁴. Scanning probe capacitance spectroscopy was able to resolve the 2D distribution of silicon atoms in a delta-doped plane in GaAs with a spatial resolution of a few nanometres⁴⁵.

Scanning tunnelling microscopy (STM) performed on the cleaved edge of a semiconductor crystal remains the most powerful technique to observe single impurities. Even in some of the first measurements using this technique, individual Si donors in GaAs (ref. 46) and Zn acceptors in GaAs (ref. 47) were clearly recognized. The local tip-induced band bending allowed the observation of these impurities in their neutral as well as their charged state. Cross-sectional scanning tunnelling microscopy (XSTM) analysis of Mn acceptors in their neutral state made it possible to analyse and understand the anisotropic charge distribution of the hole bound to the Mn acceptor⁴⁸ (see Fig. 2d). By now, spectroscopic details and the atomically precise 3D position of individual impurities can be determined⁴⁹. Unfortunately the XSTM technique is mainly limited to the natural (110) cleavage plane of III-V and II-VI semiconductor materials.

In conclusion, the most advanced techniques at the moment for observing single impurities are optical spectroscopy (especially for NV centres in diamond), transport spectroscopy in silicon nanomaterials, and XSTM for impurities in III-V and II-VI materials. The STM technique shows great promise because of its atomic resolution, wavefunction imaging and charge manipulation possibilities and the prospects for a combined electric, magnetic and optical analysis. Obtaining magnetic information, such as spin detection, on a single impurity remains a considerable challenge for STM, but recently the first successful analysis of a magnetic Fe impurity in the surface layer of InSb has been reported⁵⁰. Additional interesting approaches in this respect are local ESR and STM-induced luminescence. Examples of observational challenges are related to the detection and manipulating of single mobile and interstitial impurities⁵¹.

Modelling of impurity states

The marked effect of impurities on the properties of semiconductors motivated intense theoretical investigation into their properties early in the history of the field. Almost immediately, the essential character of impurity states was proposed, as localized states within a bandgap⁵². An expansion of the wavefunction in single-particle localized (Wannier) states, producing a recognizable effective-mass equation for shallow, Coulombic, bound states, was performed barely a decade⁵³ after the derivation of the Schrödinger equation. This approach was subsequently placed on a solid formal footing even when many-body effects were considered⁵⁴. Strong, short-range potentials, which generate deep levels within the gap, can be efficiently treated using Green's function techniques to determine the structure near the impurity⁵⁵.

In III-V zincblende semiconductors these potentials originate from an on-site potential from the impurity atom and hybridization between the tetrahedrally coordinated dangling bonds of the surrounding host and the orbitals of the impurity atom⁵⁶. For transition-metal substitutional dopants in III-V zincblende semiconductors, the partially filled *d* orbitals of the impurity atom will split into a tightly bound set of orbitals corresponding to the E irreducible representation of the tetrahedral point group, which have poor overlap with dangling bonds of the nearest-neighbour host atoms, and an extended set of orbitals of *p*-like symmetry (corresponding to the T₂ irreducible representation), which overlap well with the host⁵⁷. This symmetry-based analysis of the orbitals, introduced in a tight-binding basis^{56,57}, applies equally well to calculations of such deep levels performed with density functional theory⁵⁸. The symmetry of the bonding in the crystal dominates the wavefunction symmetry of these substitutional dopants^{48,59} (Fig. 3), with a smaller, but identifiable, effect of spin-orbit interactions^{60,61}. Symmetry analysis also provides the low-energy Hamiltonian for strain⁶² and electric fields⁶³ acting on the impurity state, but quantitative values for the resulting electronic energies require a calculation based on one of the above methods.

Internal transitions among the electronic states of the impurity can be detected in a variety of ways in macroscopic ensembles, but

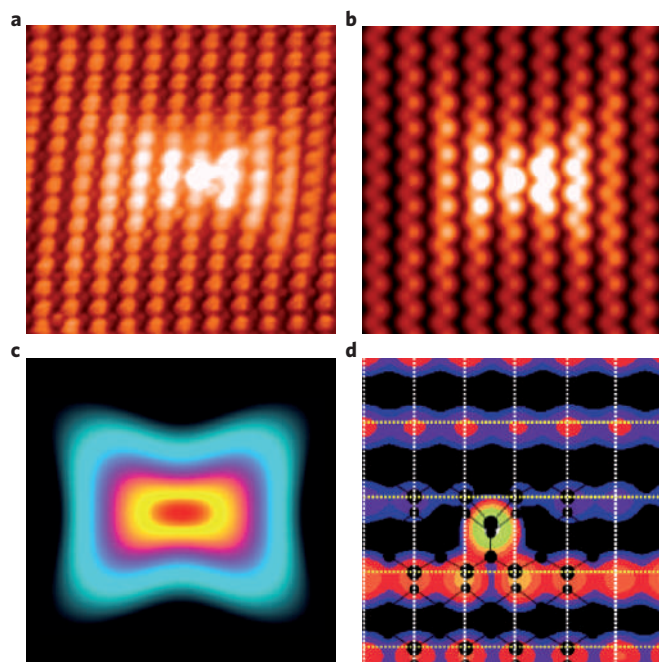


Figure 3 | Modelling of impurity states. Comparison of **a**, the charge distribution around a single Mn acceptor in GaAs as observed by STM with the charge distribution for the same defect in GaAs as obtained by **b**, tight-binding model calculations and **c**, effective-mass model calculations (after ref. 48). **d**, The charge distribution as calculated by density functional theory for a Mn atom in the surface of InAs. The scale for **a**, **b** and **d** is set by the distance between As rows, which is 0.57 nm. The rows run vertically in **a** and **b**, and horizontally in **d**. The image in **c** is 5 nm × 5 nm. Images used with permission from: **a-c**, ref. 48, © 2004 APS; **d**, ref. 67, © 2007 ACS.

have recently begun to be observable in the single-impurity limit. Calculations of the excited electronic states for Mn dopants⁵⁹ have been recently confirmed⁴⁹ for Mn in InAs. Symmetry analysis of the orbitals involved in the NV centre in diamond^{64,65} has proved similarly useful in understanding the electronic and optical transitions among electronic levels associated with this defect centre, including in the presence of strain. These calculations clarify the origin of the fluorescence transitions that are crucial to observing single-impurity dynamics in diamond. However, in the absence of atomically resolved measurements of the wavefunctions of these levels, the accuracy of these models for the electronic wavefunctions is unknown.

Each of the above approaches is particularly advantageous for some impurity–host combinations, and disadvantageous for others. For shallow impurities, whose wavefunctions extend over millions of lattice sites, calculations on an atomistic basis are currently computationally intractable, and the effective mass theory is formally correct from a many-body perspective, so it is the method of choice. Calculations using density functional theory are commonly limited to ~100 atoms, and thus cannot simulate more than the very near vicinity of a single impurity. For deep levels, however, in which the potential is restricted to within a couple of lattice spacings of the impurity, these short-range approaches can be accurate. Additional challenges arise when the impurity is taken out of the high-symmetry configuration it occupies in the bulk crystal and is placed in a more complex environment, such as the confinement of a quantum well or dot, or an applied external electric field.

Creation of single-impurity structures

The controlled creation of single-impurity devices is one of the greatest challenges in this field. Most single-impurity research up to now has been performed on impurities randomly selected by either

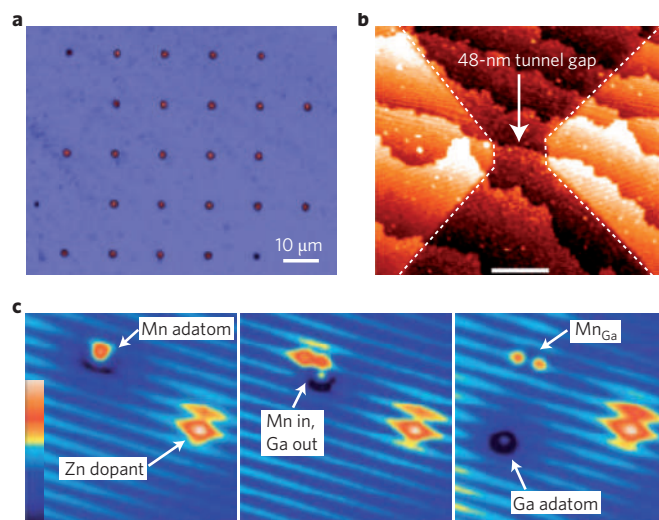


Figure 4 | Controlled incorporation of impurities. The creation of controlled dopant distributions has been achieved for **a**, single N atoms in diamond by using an ion-implanter that uses a narrow aperture in a scanning probe tip to define the implantation spot; **b**, a tunnel gap (darker) separates two P-doped source and drain regions (lighter) of Si, created by local STM-induced hydrogen removal and from a hydrogen-passivated Si surface (scale bar 50 nm); and **c**, single Mn acceptors in GaAs by STM manipulation of Mn atoms on the GaAs surface and their STM-induced incorporation in the GaAs surface layer; the Zn dopant serves as a reference point in the three images. Reprinted with permission from: **a**, ref. 68, © 2009 AIP; **b**, ref. 77, © 2007 Wiley; **c**, ref. 72, © 2006 NPG.

optical microscopy or STM, or on impurities that were accidentally present in the device structure. A natural approach to isolate a single impurity from the background is to trap the impurity in a quantum well³² or a quantum dot^{34,66} via growth kinetics. More control is possible with advances in ion implantation, which have made it possible to implant single impurities one by one with a lateral accuracy of about 20 nm due to straggling of the implanted ions⁶. Single-impurity implantation has already been used to create active devices that involve two phosphorus atoms in silicon⁶⁷, but the functionality of this device was restricted by the limited accuracy of the implantation technique. In the active field of NV centres in diamond, two teams^{68,69} have developed a technique to implant single N atoms in diamond, with a final accuracy of about 20 nm, by collimating a low-dose ion beam of an ion implanter through a small aperture (<100 nm) in the cantilever of an atomic force microscope (see Fig. 4a). According to a recent estimate²⁷, this could be sufficient to build controlled structures containing coherently coupled NV centres via magnetic dipole interactions. However, to couple the NV centres efficiently through overlap of the electronic wavefunction of the defect centres would require a spacing of a few nanometres, suggesting that further improvements in the implantation technique are desirable.

The atomic resolution possible with STM has, for some years, suggested its use as an atomically accurate fabrication tool⁷⁰. Recently, nearly atomic resolution in single-impurity implantation in the surface layer of GaAs has been demonstrated by STM-induced substitution of Mn, Fe and Co in a (110) GaAs or InAs surface^{71–73}. The resolution is limited to about 1 or 2 nm owing to randomness of the substitution process when the voltage pulse between the surface impurity and the STM tip is applied. The process is, however, reversible, which allows continued attempts until the intended placement is achieved. This approach has permitted exploration of the spin–spin interaction between two Mn atoms⁷². A first result with the creation of heterogeneous impurity molecules in the GaAs surface⁷⁴

shows great prospects for further progress in controlling spin–spin interaction at the atomic scale. The options are enormous when one can start to build heterogeneous impurity molecules composed of different impurity species that are arranged in artificial patterns. The prospects for this kind of molecular impurity physics might be as rich as those in chemistry. The cleaved (110) surface, however, is currently remote from a device environment, as cleaved-edge overgrowth would be required to fix the impurities stably into a room-temperature device.

A more direct approach to single-dopant device fabrication has been to work with a silicon surface terminated with hydrogen. An STM tip is then used to remove hydrogen atoms locally. After this step the surface is exposed to phosphine, which bonds only with the exposed silicon⁷⁵. Subsequent stripping of the hydrogen from the surface and the phosphine molecules⁷⁶, followed by silicon overgrowth, allows for the creation of embedded arrangements of P atoms (see Fig. 4b). Although the final goal of placing a single P dopant in a functional silicon device has not yet been reached, all process steps have been demonstrated and functional nanocircuitry based on homogeneously doped areas has been created⁷⁷. The ultimate resolution in this case is mainly determined by the chemistry during the hydrogen removal.

Although the creation of artificial arrangements of impurities in a semiconductor by STM is rapidly approaching the level of atom manipulation on metals, no matter how exquisite this work might be, it would be far more elegant if we could find self-assembly processes that arranged the impurities spontaneously. Other classes of interesting defects that remain to be explored are bistable and mobile impurities, because they would allow for even more complex functionalities.

Interaction with single impurities

Manipulation and sensing of a single impurity is determined by its interaction with the environment. This consists, first and foremost, of the host crystal, but it also encompasses components such as

confinement potentials, electric and magnetic fields, photons and phonons, and other impurities nearby. Understanding the interaction of a single impurity with this complex environment is essential because it allows tuning of the impurity properties as well as state manipulation and sensing. The environment might also be detrimental, for instance limiting the coherence and lifetime of the impurity state. Interaction of an impurity with the host material is, of course, fundamentally embedded into the modelling described above. We therefore focus here on the interaction of an impurity with the other components of the environment.

To make use of single impurities in an active device we need to be able to manipulate the impurity state through interaction with the externally controlled portions of the environment. Gate-induced ionization of impurities, which lies at the basis of most electronic devices, is probably the simplest operation. Ionizing a single impurity requires either a very low density of impurities in the device structure or a nanoscale gate. The latter has been demonstrated by using an STM to ionize single impurities⁷⁸ and measure for instance the binding energy of an electron to a Si donor close to the interface between GaAs and the vacuum⁷⁹. Charge manipulation on single NV centres has not yet been shown. The most apparent effect of an impurity interacting with the electrical field distribution is, of course, its ionization, but the more subtle effects occurring before ionization, such as the effect of an electric field on the binding energy and the wavefunction, are very useful and interesting. The Stark effect on impurities has been analysed experimentally for NV centres in diamond⁸⁰ and P donors in a silicon nano-MOSFET⁸¹. Extensive calculations for the latter case, in which the donor bound electron is not removed by the ionization process but remains trapped in the combined potential of the donor and the Si/SiO interface, have also been reported⁸². It has been suggested that intervalley coupling can have profound effects on the quantum operation of a P-donor in silicon⁸³.

More importantly from the viewpoint of quantum processing, it is very useful to find ways of coupling local electric fields to the spin properties of an impurity. Such an interaction is predicted for a

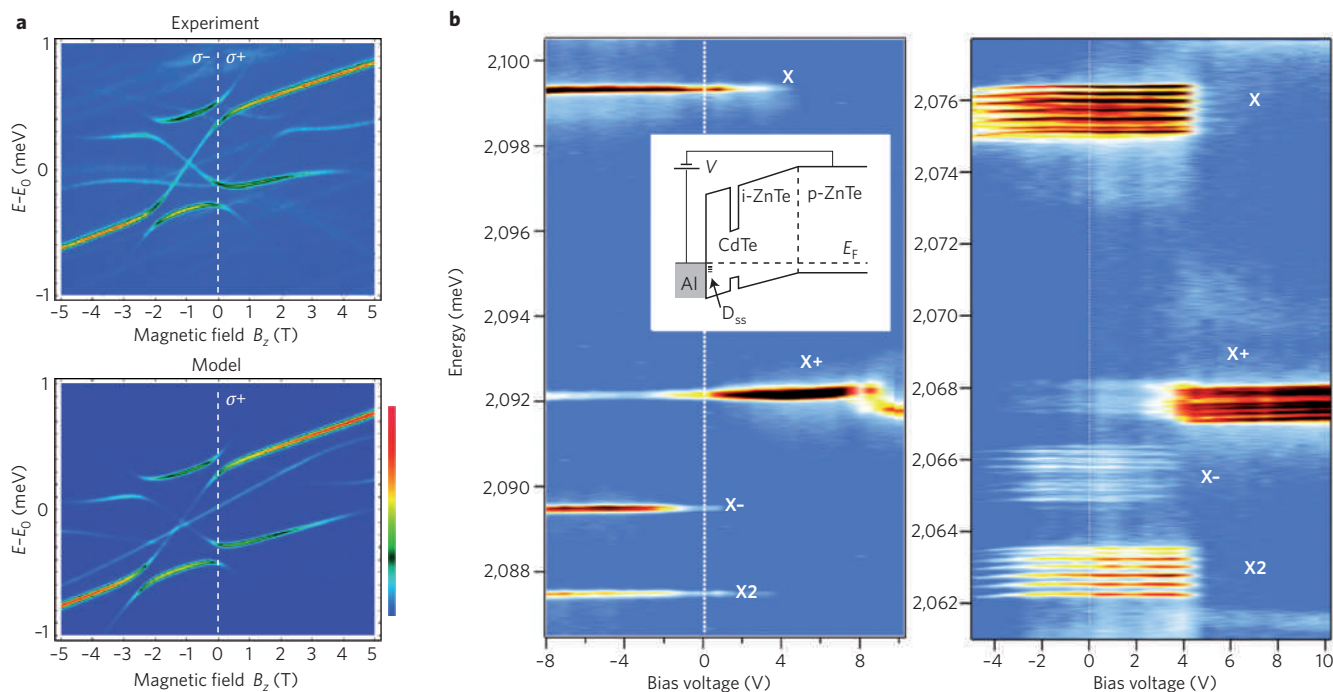


Figure 5 | Optical spectroscopy of single impurities. Spectral analysis by confocal microscopy of: **a**, The manipulation of a single Mn acceptor in a InAs quantum dot in GaAs and by an external magnetic field. E is photon energy; $E_0 = 1.355$ eV; σ indicates the photon polarization. **b**, The interaction of a single Mn impurity in a CdTe quantum dot with a single additional, gate-voltage-induced, charge carrier confined in the same quantum dot. The indices indicate the various charged and neutral exciton complexes. Reprinted with permission from: **a**, ref. 89, © 2009 APS; **b**, ref. 88, © 2005 Elsevier.

Mn acceptor⁶³ and a hydrogen donor⁸⁴ in GaAs; in both these cases, spin-orbit interaction is responsible for the coupling between the external electric field and the spin properties. Experimentally, Stark tuning of the spin of an electron bound to a Sb impurity⁸⁵ and the electrical-field-induced Rabi flops of P spin⁸⁶ in silicon have been reported recently. Another approach to controlling the magnetic properties of an impurity is used for magnetic Mn atoms in a CdTe quantum dot. In such a dot the interaction of a single Mn impurity with a finite number of charge carriers, controlled by external gating and residing in the dot, determines the magnetic properties of this nanosystem⁸⁷ (Fig. 5b).

Optical excitation is a very appropriate way to manipulate either an impurity or its environment. Excitons bound weakly to an impurity retain their host character, such as those bound to N-acceptors in ZnSe quantum wells¹³. Photoionization can also be used as a tool to change the charge state of a strongly bound NV centre⁸⁸ or the population of a quantum dot that interacts with the Mn-impurity inside^{87,89} (Fig. 5a). Optical excitation of NV centres has also been used to bring it into an excited state²⁹ where the spin properties are to be modified. The environment of the NV centre affects its properties through local strain fluctuations²⁹ or the spins of neighbouring impurities³⁰. In the latter case the spin coherence can be improved by polarizing the spin bath of the other impurities in the neighbourhood of the NV centre⁹⁰.

The magnetic field is another convenient external parameter to couple to impurities and control magnetic properties such as nearby nuclear spins, or the spin of the donor or acceptor bound charge carrier. Notable in this respect are recent calculations of the local density of states and spin anisotropy of Mn impurities close to a GaAs (110) vacuum interface^{60,61}. These results predict the possibility of detecting the spin orientation of a single Mn impurity by STM topography. Dynamic magnetic fields are, however, not easily available in devices.

Strain is another environmental parameter that cannot easily be actively manipulated but is certainly very often an important component of the impurity environment. The effect of strain on an effective mass acceptor state can be rather complex but is by now well understood⁹¹. Impurities present near⁶² or in⁸⁹ a strained self-assembled quantum dot have been studied experimentally, and it has been shown that strain due to the surface reconstruction is an essential ingredient in understanding the behaviour of impurities below a reconstructed surface^{61,92,93}. The latter result applies to all impurities observed by XSTM, especially the shallow impurities that couple most strongly with the surface. The above strains are static; dynamic strain, such as from a phonon, provides a potential additional method of manipulating single-dopant electronic structure.

The advantage of semiconductors is the ease in creating low-dimensional systems such as quantum wells and quantum dots, and this motivates a study of the confinement effect on impurity states. For shallow impurities the situation is considered rather straightforward, as charge carriers just experience the combined effect of the impurity potential and the additional confinement potential⁹⁴. However, in the case of deep impurities, such as Mn in a quantum well, the situation becomes less straightforward⁹⁵. Potential barriers that include vacuum or oxide interfaces are even more complex, as shown for instance for P donors in Si colloidal dots and nano-MOSFETS, for which the change of localization is dominated by a reduction of dielectric screening^{96,97}, and at vacuum-semiconductor interfaces, where a recent study of Si impurities close to the GaAs-vacuum interface showed that effective mass theory breaks down⁷⁹ and strain induced by surface reconstruction plays an essential role^{61,92,93}. If the behaviour of impurities is well understood, however, they could act as a local sensor to probe local properties such as the strain distribution in or near a quantum dot^{62,89} or a strained interface⁹². A more complete understanding of impurities in a confining potential and near an interface is thus much needed.

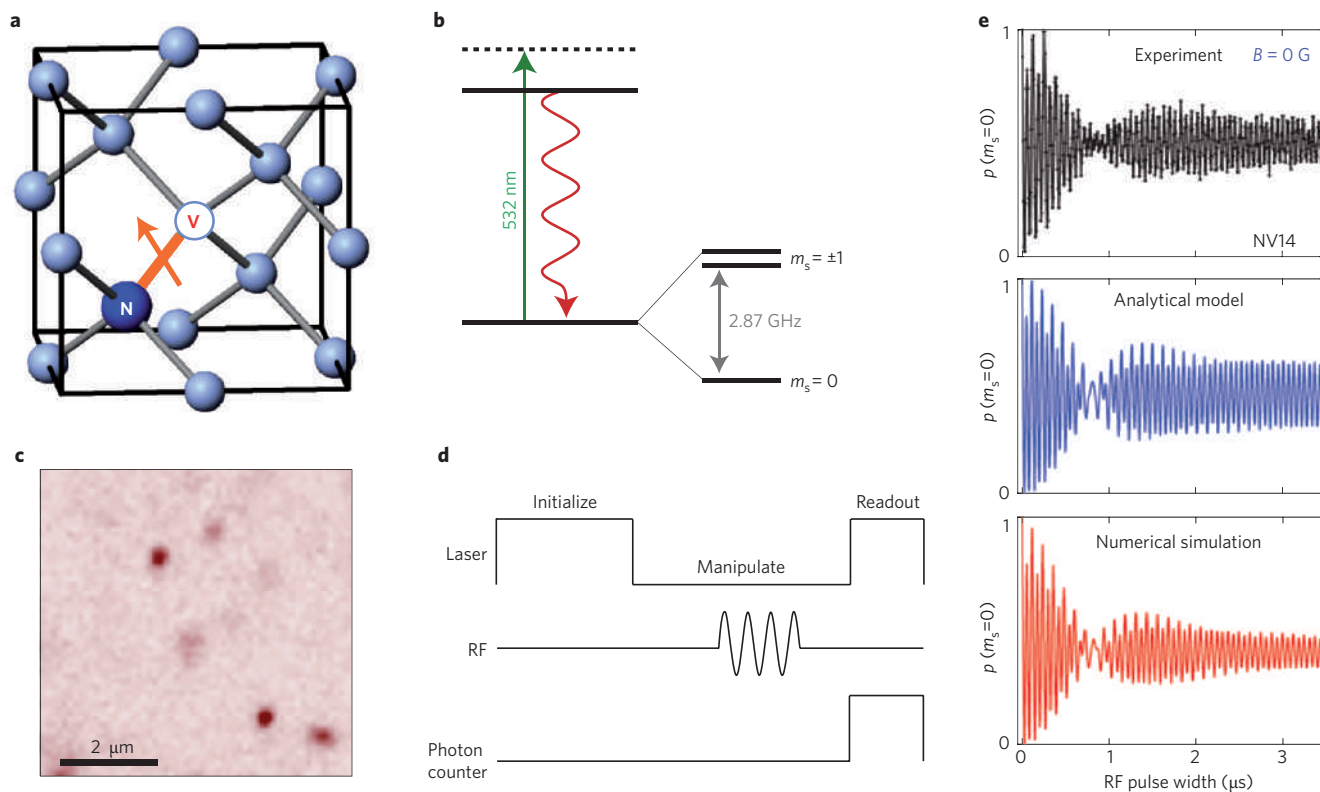


Figure 6 | NV centre manipulation. **a**, Structure of NV centre in diamond; **b**, energy level structure; **c**, optical imaging of NV centres; **d**, pulse sequence for spin manipulation; **e**, measurements of response of the single impurity to the pulse sequence, along with theoretical results. $p(m_s = 0)$ indicates the probability of the spin in the zero spin-projection state. Reprinted with permission from ref. 101, © 2008 APS.

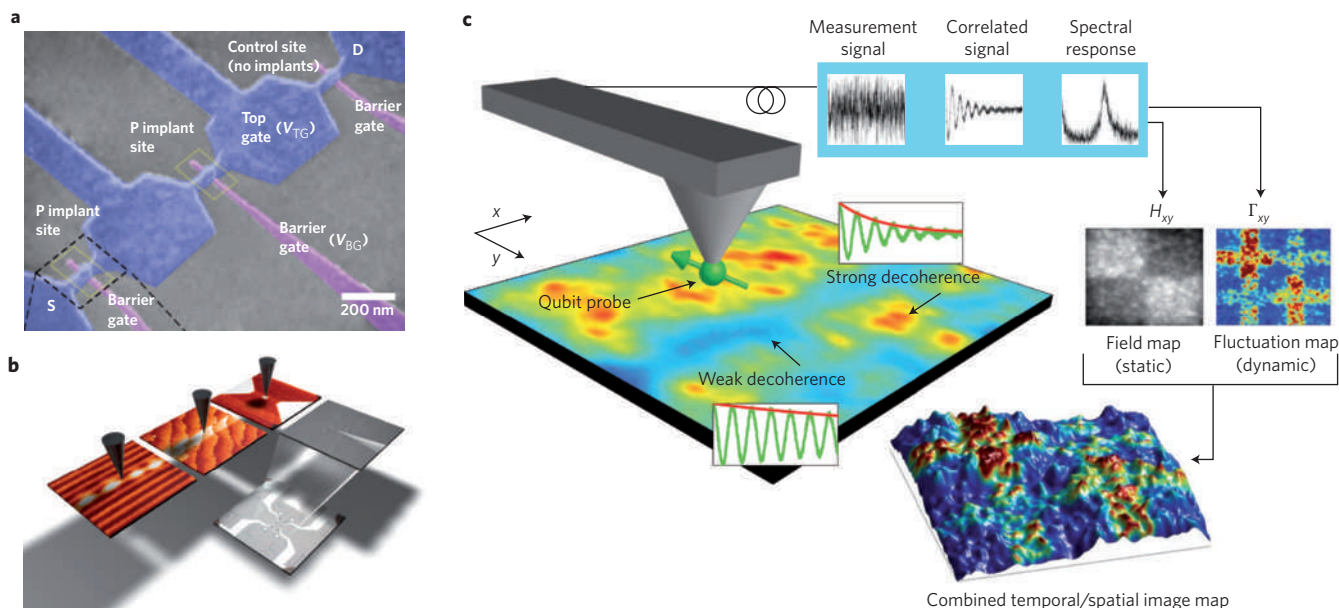


Figure 7 | Single impurity devices. Examples of created and proposed single-impurity devices. **a**, Nano-FET with locally implanted single P atoms, which allowed the electron states and transport properties of a single P atom to be studied. **b**, Proposed scheme to create single P atom devices in silicon by hydrogen passivation of the Si surface, followed by STM-tip-induced local removal of the hydrogen to create the contact pads and to control the position of a single P atom between the contact pads. **c**, Proposed scanning probe setup that uses a single NV centre at the apex of the scanning probe tip to measure the spatial and temporal quantum coherence of objects under the tip. Reprinted with permission from: **a**, ref. 111, © 2010 ACS; **b**, ref. 77, © 2007 Wiley; **c**, ref. 110, © 2009 IOP.

The study of impurity–impurity interaction is still an open field, and thus far only some first results for isolated Mn–Mn pairs have been published^{72,98} and some first results on the spin lifetime of small clusters of Mn acceptors in a GaAs quantum well³². Studying such impurity–impurity interaction is not only essential for the comprehension of impurity band formation, which is an important issue in magnetic semiconductors such as GaMnAs, but likely to be rewarding for the understanding and use of entangled impurity states, and will also allow us to understand how to read out the spin state of one impurity by probing another coupled impurity.

Single-impurity devices

To meet the ultimate challenge in single-impurity physics, the creation of functional single-impurity devices for quantum information processing, several proposals have been presented and investigated. These concepts and their (partial) realizations can broadly be split into optical and electronic devices. NV centres in diamond and other optically active defects in semiconductors fall into the category of optical devices, whereas those based on spin preparation, manipulation and detection by local gates and single-electron transistors fall into the category of electronic devices.

A first step towards the application of single impurities and defects in optical devices involves the triggered emission of single photons. This has been demonstrated successfully for N-acceptors in ZnSe quantum wells¹³ and NV centres in diamond¹⁴. This is a first step towards using single impurities as a single-photon source for quantum key distribution in quantum secure communication. Optical probing³³ and orientation³⁵ of a single Mn spin has been shown for an isolated Mn atom in a CdTe quantum dot. Spectacular progress has been seen in the past few years in quantum information processing on NV. This has been shown by a successful preparation of the spin state of a NV centre by means of optical excitation, manipulation by RF fields and optical readout^{28,99–102} (see Fig. 6). Although the NV centre is a point defect and its electron spin is mostly localized at the defect site, some of its electron spin density is distributed over the nearest-neighbour carbon atoms. As a

result, substantial hyperfine and dipolar coupling are present owing to single nuclei localized close to the defect. The coupling has been used to control the nuclear spin on a single C nucleus to realize a two-qubit conditional quantum gate¹⁰³. By controlling the nuclear spin on two individual C nuclei in a nearest-neighbour position, the entanglement of their spins was shown¹⁰⁴. In another approach it has been shown that one can probe isolated N spins using an NV centre¹⁰⁵. Building on such successes in this rapidly expanding field, new device concepts based on NV centres, for instance a quantum repeater¹⁰², are currently proposed. Interestingly, a single NV centre has also been used as a probe to sense non-invasively the magnetic field distribution at the nanoscale^{106–109}, and recently the idea has been put forward to use a single NV centre in a scanning quantum decoherence microscope¹¹⁰ (Fig. 7c).

A number of electronic device concepts have been suggested for the quantum manipulation of a single impurity. Kane proposed that information could be encoded onto the nuclear spins of P atoms in silicon electronic devices⁷. Logical quantum operations on the individual nuclear spins could then be performed by using externally applied electric fields that control the electronic bound state around the P atom, which couples both to other P atoms and to the nuclear spin. The nuclear spins would then be read out by a charge-based method using spin-polarized electrons that directly probed the electronic bound state around the P atoms. Vrijen *et al.* proposed a SiGe transistor that exploits band-structure engineering to sense and control a single-donor electron spin⁸. It is proposed that by applying a gate bias, one- and two-qubit operations could be performed, because the electrical field could be used to pull the electron wavefunction away from the dopant ion into layers of different composition having a different *g*-factor. Owing to the variation of the *g*-factor, this displacement changes the spin Zeeman energy, allowing qubit operations. Readout of the spin information would be performed indirectly by a charge-based approach using a current flowing close to the impurity, which owing to the Pauli exclusion principle can only bind a second electron when this has opposite spin to the first. Whereas both previous schemes are based on spin

manipulation, Hollenberg *et al.* proposed a completely charge-based quantum computation approach⁹. In their scheme, two interacting doping atoms, of which only one is ionized, act as the qubit for the quantum operations. Local electric fields control the qubit, and single-electron transistors are proposed for the readout.

Important steps towards the realization of electronic single-impurity devices for quantum processing in silicon have been made in the past few years, but many challenges lie ahead. Single ion implantation has undoubtedly been one of the first important steps toward single-impurity devices in silicon⁶. In such implanted devices, an ordered distribution of single impurities lowers the threshold voltage of the FET, and the device-to-device fluctuations are smaller. Single-ion implantation has been used to create silicon devices that use single-electron transistors to demonstrate the controlled charging of pairs of P atoms in the active channel of a silicon-based structure⁶⁷. The results showed that the relaxation time for the charge state at millikelvin temperature, which is dominated by charge fluctuations occurring in the background and phonon emission, can be up to several milliseconds long. Very recently, transport spectroscopy on a single P donor in silicon has been demonstrated in a nanoscale transistor where the P donor was implanted¹¹¹ (Fig. 7a). As described before, STM-controlled placement of P and subsequent overgrowth by silicon⁷⁷ (Fig. 7b) is the most promising method at the moment. It has not yet produced a device operating on a single P impurity, but it is anticipated that this approach will open the door for controlled scaling of silicon devices towards the single-donor limit.

The future of solotronics

Many of the advances described above for single impurities in semiconductors have been mirrored, either earlier or later, by similar advances in the physics of single-electron semiconductor quantum dots, either electrostatic or self-assembled. Quantum dots offer the advantage that they come in innumerable variety, depending on details of their construction; this is also their disadvantage. Control of gate design and voltage, for electrostatic dots, or growth parameters, for self-assembled dots, offers a vast parameter space for designing a dot for a given purpose. However, no quantum dot is precisely like any other. Examples of parallel development include spin manipulation and readout of charge and spin for quantum information processing in lithographic quantum dots¹¹², and applications of self-assembled quantum dots¹¹³ to single-photon generation¹¹⁴ and quantum information processing^{115,116}.

Single impurities are perhaps further ahead than quantum dots in areas where all-optical techniques can be used, but are behind quantum dots when gates are essential. The room-temperature quantum coherence of NV centres in diamond, along with optical manipulation and magnetic dipolar coupling, permits the potential realization of a wide variety of quantum device functionality, including quantum computation. However, it remains difficult to gate these centres electrically. If the gating problem can be solved for diamond, then other types of electronic devices relying on single impurities can be expected to progress rapidly. In other semiconductor-dopant systems, where gating has been achieved, single impurities have much lower optical emission rates and more rapid saturation than single centres in diamond or single quantum dots. However, quite a few important advantages are still to be expected when single impurities are used rather than quantum dots in these materials. For instance, the spin coherence lifetime of self-assembled quantum dots is limited by the interaction of the dot with carriers in the omnipresent wetting layers, whereas doping atoms can be introduced as truly isolated objects. Extremely long spin lifetimes have already been reported for P in silicon¹¹⁷, which could be even further enhanced in the case that the environmental spin bath is optically spin-polarized¹⁰¹, and much higher densities of emitters can be obtained by impurities compared with self-assembled quantum dots. The creation of single-photon

emitters is normally realized by quantum dots that emit by chance at the mode of the cavity; in contrast, impurities have excellent reproducible emission energies. Single impurities also do not have the major drawback of electrostatic dots — their inability to emit photons. Finally, it may be possible to find spin centres in materials other than diamond that share diamond's exceptionally long spin coherence times at room temperature.

Measurement of the full electronic spectrum of an impurity in a semiconductor, including excited states and spatially mapped wavefunctions, is a goal that seems within reach. Observations of the electronic spectrum, and the dynamics of carriers within the impurity states, are well advanced at room temperature for optical probes of NV centres in diamond. For spatially mapped wavefunctions, STM on cleaved (110) surfaces has provided extensive information about a variety of impurities and hosts. Optical single-quantum devices, such as for quantum information processing, are thus furthest advanced for NV centres in diamond, whereas single-impurity effects on device transport are most developed for silicon, germanium, III-V and II-VI semiconductors. Challenges for diamond include gating, atomically resolved imaging of dopants, and the control of electronic interactions among many interacting NV centres. A challenge for other semiconductors is the achievement of stable single-impurity properties, including methods of observing a non-equilibrium/quantum coherent state, at room temperature.

The prospects for electronic single-impurity devices realized in silicon, III-V or II-VI may be bright in the long run because these semiconductor materials allow for an almost infinite choice in host materials, allow the inclusion of a confinement potential such as quantum wells and quantum dots in the design, and have a mature multilayer and photonic crystal cavity technology, a wider range of doping impurities and the possibility of creating conduction channels and single-electron transistors close to the impurity. It is also a great advantage that entangled impurity states could be realized with impurities having a relatively large separation in the range of 10 to 100 nm, and that impurities can be reproducibly positioned on the atomic scale. As advances continue in observation, modelling, manipulation, creation and devices, this field of solotronics seems to be progressing to the point where the essential element of a device is a single dopant atom, contacted with leads and gates, or optically addressed. This will bring the semiconductor device community to the end of the road in device miniaturization.

References

- Pauli, W. *1930–1935 Scientific Correspondence with Bohr, Einstein, Heisenberg and Others* Vol. 2, 4 (Springer, 1985).
- Ralls, K. S. *et al.* Discrete resistance switching in submicrometer silicon inversion layers: Individual interface traps and low-frequency ($1/f$) noise. *Phys. Rev. Lett.* **52**, 228–231 (1984).
- Dekker, C. *et al.* Spontaneous resistance switching and low-frequency noise in quantum point contacts. *Phys. Rev. Lett.* **66**, 2148–2151 (1991).
- Neugroschel, A., Sah, C.-T. & Carroll, M. S. Random telegraphic signals in silicon bipolar junction transistors. *Appl. Phys. Lett.* **66**, 2879–2881 (1995).
- Asenov, A., Brown, A., Davies, J., Kaya, S. & Slavcheva, G. Simulation of intrinsic parameter fluctuations in decananometer and nanometer-scale MOSFETs. *IEEE Trans. Electron. Dev.* **50**, 1837–1852 (2003).
- Shinada, T., Okamoto, S., Kobayashi, T. & Ohdomari, I. Enhancing semiconductor device performance using ordered dopant arrays. *Nature* **437**, 1128–1131 (2005).
- Kane, B. E. A silicon-based nuclear spin quantum computer. *Nature* **393**, 133–137 (1998).
- Vrijen, R. *et al.* Electron-spin-resonance transistors for quantum computing in silicon-germanium heterostructures. *Phys. Rev. A* **62**, 012306 (2000).
- Hollenberg, L. C. L. *et al.* Charge-based quantum computing using single donors in semiconductors. *Phys. Rev. B* **69**, 113301 (2004).
- Kurtsiefer, C., Mayer, S., Zarda, P. & Weinfurter, H. Stable solid-state source of single photons. *Phys. Rev. Lett.* **85**, 290–293 (2000).
- Muller, A. *et al.* Time-resolved photoluminescence spectroscopy of individual Te impurity centers in ZnSe. *Phys. Rev. B* **73**, 081306 (2006).
- Ikezawa, M., Sakuma, Y. & Masumoto, Y. Single photon emission from individual nitrogen pairs in GaP. *Jpn J. Appl. Phys.* **46**, L871–L873 (2007).
- Strauf, S. *et al.* Quantum optical studies on individual acceptor bound excitons in a semiconductor. *Phys. Rev. Lett.* **89**, 177403 (2002).

14. Beveratos, A. *et al.* Room temperature stable single-photon source. *Eur. Phys. J. D* **18**, 191–196 (2002).
15. Xiao, M., Martin, I., Yablonovitch, E. & Jiang, H. W. Electrical detection of the spin resonance of a single electron in a silicon field-effect transistor. *Nature* **430**, 435–439 (2004).
16. Dellow, M. *et al.* Resonant tunneling through the bound-states of a single donor atom in a quantum-well. *Phys. Rev. Lett.* **68**, 1754–1757 (1992).
17. Deshpande, M., Sleight, J., Reed, M., Wheeler, R. & Matyi, R. Spin splitting of single 0D impurity states in semiconductor heterostructure quantum wells. *Phys. Rev. Lett.* **76**, 1328–1331 (1996).
18. Vdovin, E., Khanin, Y., Eaves, L., Henini, M. & Hill, G. Spin splitting of X-valley-related donor impurity states in an AlAs barrier. *Phys. Rev. B* **71**, 195320 (2005).
19. Sakai, J. *et al.* Probing the wave-function of quantum-confined states by resonant magnetotunneling. *Phys. Rev. B* **48**, 5664–5667 (1993).
20. Jouault, B. *et al.* Single-impurity tunneling spectroscopy to probe the discrete states of a two-dimensional electron gas in a quantizing magnetic field. *Phys. Rev. B* **73**, 155415 (2006).
21. Calvet, L. E., Wernsdorfer, W., Snyder, J. P. & Reed, M. A. Transport spectroscopy of single Pt impurities in silicon using Schottky barrier MOSFETs. *J. Phys. Condens. Matter* **20**, 374125 (2008).
22. Sellier, H. *et al.* Transport spectroscopy of a single dopant in a gated silicon nanowire. *Phys. Rev. Lett.* **97**, 206805 (2006).
23. Roberts, G. *et al.* Voltage-controlled sharp-line electroluminescence in GaAs–AlAs double-barrier resonant-tunneling structures. *Phys. Rev. B* **58**, R4242–R4245 (1998).
24. Francoeur, S., Klem, J. & Mascarenhas, A. Optical spectroscopy of single impurity centers in semiconductors. *Phys. Rev. Lett.* **93**, 067403 (2004).
25. Gruber, A. *et al.* Scanning confocal optical microscopy and magnetic resonance on single defect centers. *Science* **276**, 2012–2014 (1997).
26. Rittweger, E., Han, K. Y., Irvine, S. E., Egging, C. & Hell, S. W. STED microscopy reveals crystal colour centres with nanometric resolution. *Nature Photon.* **3**, 144–147 (2009).
27. Balasubramanian, G. *et al.* Ultralong spin coherence time in isotopically engineered diamond. *Nature Mater.* **8**, 383–387 (2009).
28. Jelezko, F. & Wrachtrup, J. Single defect centres in diamond: A review. *Phys. Status Solidi A* **203**, 3207–3225 (2006).
29. Fuchs, G. D. *et al.* Excited-state spectroscopy using single spin manipulation in diamond. *Phys. Rev. Lett.* **101**, 117601 (2008).
30. Hanson, R. & Awschalom, D. D. Coherent manipulation of single spins in semiconductors. *Nature* **453**, 1043–1049, Jun (2008).
31. Neumann, P. *et al.* Excited-state spectroscopy of single NV defects in diamond using optically detected magnetic resonance. *New J. Phys.* **11**, 013017 (2009).
32. Myers, R. C. *et al.* Zero-field optical manipulation of magnetic ions in semiconductors. *Nature Mater.* **7**, 203–208 (2008).
33. Besombes, L. *et al.* Probing the spin state of a single magnetic ion in an individual quantum dot. *Phys. Rev. Lett.* **93**, 207403 (2004).
34. Kudelski, A. *et al.* Optically probing the fine structure of a single Mn atom in an InAs quantum dot. *Phys. Rev. Lett.* **99**, 247209 (2007).
35. Gall, C. L. *et al.* Optical spin orientation of a single manganese atom in a semiconductor quantum dot using quasiresonant photoexcitation. *Phys. Rev. Lett.* **102**, 127402 (2009).
36. Rugar, D., Budakian, R., Mamin, H. J. & Chui, B. W. Single spin detection by magnetic resonance force microscopy. *Nature* **430**, 329–332 (2004).
37. Manassen, Y., Hamers, R. J., Demuth, J. E., and A. J. Castellano, J. Direct observation of the precession of individual paramagnetic spins on oxidized silicon surfaces. *Phys. Rev. Lett.* **62**, 2531–2534 (1989).
38. Durkan, C. & Welland, M. E. Electronic spin detection in molecules using scanning-tunneling-microscopy-assisted electron-spin resonance. *Appl. Phys. Lett.* **80**, 458–460 (2002).
39. Sainoo, Y., Isshiki, H., Shahed, S. M. F., Takaoka, T. & Komeda, T. Atomically resolved Larmor frequency detection on Si(111)-7 × 7 oxide surface. *Appl. Phys. Lett.* **95**, 082504 (2009).
40. Voyles, P., Grazul, J. & Muller, D. Imaging individual atoms inside crystals with ADF-stem. *Ultramicroscopy* **96**, 251–273 (2003).
41. van Benthem, K. *et al.* Three-dimensional imaging of individual hafnium atoms inside a semiconductor device. *Appl. Phys. Lett.* **87**, 034104 (2005).
42. Kelly, T. F. & Miller, M. K. Invited review article: Atom probe tomography. *Rev. Sci. Instrum.* **78**, 031101 (2007).
43. Topinka, M. *et al.* Imaging coherent electron flow from a quantum point contact. *Science* **289**, 2323–2326 (2000).
44. Woodside, M. & McEuen, P. Scanned probe imaging of single-electron charge states in nanotube quantum dots. *Science* **296**, 1098–1101 (2002).
45. Kuljanishvili, I. *et al.* Scanning-probe spectroscopy of semiconductor donor molecules. *Nature Phys.* **4**, 227–233 (2008).
46. Feenstra, R. M. *et al.* Cross-sectional imaging and spectroscopy of GaAs doping superlattices by scanning tunneling microscopy. *Appl. Phys. Lett.* **61**, 795–797 (1992).
47. Zheng, Z., Salmeron, M. & Weber, E. Empty state and filled state image of Zn_{Ca} acceptor in GaAs studied by scanning-tunneling-microscopy. *Appl. Phys. Lett.* **64**, 1836–1838 (1994).
48. Yakunin, A. M. *et al.* Spatial structure of an individual Mn acceptor in GaAs. *Phys. Rev. Lett.* **92**, 216806 (2004).
49. Marczinowski, F. *et al.* Local electronic structure near Mn acceptors in InAs: Surface-induced symmetry breaking and coupling to host states. *Phys. Rev. Lett.* **99**, 157202 (2007).
50. Khajetoorians, A. A. *et al.* Detecting excitation and magnetization of individual dopants in a semiconductor. *Nature* **467**, 1084–1087 (2010).
51. Wijnheijmer, A. P. *et al.* Nanoscale potential fluctuations in (Ga, Mn)As/GaAs heterostructures: From individual ions to charge clusters and electrostatic quantum dots. *Nano Lett.* **10**, 102739 (2010).
52. Wilson, A. H. The theory of electronic semiconductors. II *Proc. R. Soc. A* **134**, 277–287 (1931).
53. Wannier, G. H. The structure of electronic excitation levels in insulating crystals. *Phys. Rev.* **52**, 191–197 (1937).
54. Kohn, W. Shallow impurity states in silicon and germanium. *Solid State Phys.* **5**, 257 (1957).
55. Koster, G. F. & Slater, J. C. Wave functions for impurity levels. *Phys. Rev.* **95**, 1167–1176 (1954).
56. Hjalmarson, H. P., Vogl, P., Wolford, D. J. & Dow, J. D. Theory of substitutional deep traps in covalent semiconductors. *Phys. Rev. Lett.* **44**, 810–813 (1980).
57. Vogl, P. & Baranowski, J. M. Electronic structure of 3d-transition metal impurities in semiconductors. *Acta Phys. Polon. A* **67**, 133–142 (1985).
58. Mahadevan, P. & Zunger, A. First-principles investigation of the assumptions underlying model-Hamiltonian approaches to ferromagnetism of 3d impurities in III–V semiconductors. *Phys. Rev. B* **69**, 115211 (2004).
59. Tang, J.-M. & Flatté, M. E. Multiband tight-binding model of local magnetism in Ga_{1-x}Mn_xAs. *Phys. Rev. Lett.* **92**, 047201 (2004).
60. Tang, J.-M. & Flatté, M. E. Spin-orientation-dependent spatial structure of a magnetic acceptor state in a zincblende semiconductor. *Phys. Rev. B* **72**, 161315 (2005).
61. Strandberg, T. O., Canali, C. M. & MacDonald, A. H. Magnetic properties of substitutional Mn in (110) GaAs surface and subsurface layers. *Phys. Rev. B* **80**, 024425 (2009).
62. Yakunin, A. M. *et al.* Warping a single Mn acceptor wavefunction by straining the GaAs host. *Nature Mater.* **6**, 512–515 (2007).
63. Tang, J.-M., Levy, J. & Flatté, M. E. All-electrical control of single ion spins in a semiconductor. *Phys. Rev. Lett.* **97**, 106803 (2006).
64. Lenef, A. & Rand, S. C. Electronic structure of the NV center in diamond: Theory. *Phys. Rev. B* **53**, 13441–13455 (1996).
65. Manson, N. B., Harrison, J. P. & Sellars, M. J. Nitrogen-vacancy center in diamond: Model of the electronic structure and associated dynamics. *Phys. Rev. B* **74**, 104303 (2006).
66. Maingault, L., Besombes, L., Leger, Y., Bougerol, C. & Mariette, H. Inserting one single Mn ion into a quantum dot. *Appl. Phys. Lett.* **89**, 193109 (2006).
67. Andresen, S. E. *et al.* Charge state control and relaxation in an atomically doped silicon device. *Nano Lett.* **7**, 2000–2003 (2007).
68. Naydenov, B. *et al.* Engineering single photon emitters by ion implantation in diamond. *Appl. Phys. Lett.* **95**, 181109 (2009).
69. Weis, C. D. *et al.* Single atom doping for quantum device development in diamond and silicon. *J. Vac. Sci. Technol. B* **26**, 2596–2600 (2008).
70. O'Brien, J. *et al.* Towards the fabrication of phosphorus qubits for a silicon quantum computer. *Phys. Rev. B* **64**, 161401 (2001).
71. Song, Y. J. *et al.* Making Mn substitutional impurities in InAs using a scanning tunneling microscope. *Nano Lett.* **9**, 4333–4337 (2009).
72. Kitchen, D., Richardella, A., Tang, J.-M., Flatté, M. E. & Yazdani, A. Atom-by-atom substitution of Mn in GaAs and visualization of their hole-mediated interactions. *Nature* **442**, 436–439 (2006).
73. Richardella, A., Kitchen, D. & Yazdani, A. Mapping the wave function of transition metal acceptor states in the GaAs surface. *Phys. Rev. B* **80**, 045318 (2009).
74. Lee, D. H. & Gupta, J. A. Tunable field-control over the binding energy of single dopants by a charged vacancy in GaAs. *Science* doi:10.1126/science.1197434 (2010).
75. Schofield, S. R. *et al.* Atomically precise placement of single dopants in Si. *Phys. Rev. Lett.* **91**, 136104 (2003).
76. Wilson, H. *et al.* Phosphine dissociation on the Si(001) surface. *Phys. Rev. Lett.* **93**, 226102 (2004).
77. Ruess, F. J. *et al.* Realization of atomically controlled dopant devices in silicon. *Small* **3**, 563–567 (2007).
78. Teichmann, K. *et al.* Controlled charge switching on a single donor with a scanning tunneling microscope. *Phys. Rev. Lett.* **101**, 076103 (2008).
79. Wijnheijmer, A. P. *et al.* Enhanced donor binding energy close to a semiconductor surface. *Phys. Rev. Lett.* **102**, 166101 (2009).
80. Tamarat, P. *et al.* Stark shift control of single optical centers in diamond. *Phys. Rev. Lett.* **97**, 083002 (2006).
81. Lansbergen, G. P. *et al.* Gate-induced quantum-confinement transition of a single dopant atom in a silicon FINFET. *Nature Phys.* **4**, 656–661 (2008).
82. Rahman, R. *et al.* Orbital stark effect and quantum confinement transition of donors in silicon. *Phys. Rev. B* **80**, 165314 (2009).
83. Saraiva, A., Calderon, M., Hu, X., Sarma, S. D. & Koiller, B. Physical mechanisms of interface-mediated intervalley coupling in Si. *Phys. Rev. B* **80**, 081305 (2009).
84. De, A., Pryor, C. E. & Flatté, M. E. Electric-field control of a hydrogenic donor's spin in a semiconductor. *Phys. Rev. Lett.* **102** (2009).

85. Bradbury, F. R. *et al.* Stark tuning of donor electron spins in silicon. *Phys. Rev. Lett.* **97**, 176404 (2006).
86. Stegner, A. R. *et al.* Electrical detection of coherent ^{31}P spin quantum states. *Nature Phys.* **2**, 835–838 (2006).
87. Leger, Y., Besombes, L., Fernandez-Rossier, J., Maingault, L. & Mariette, H. Electrical control of a single Mn atom in a quantum dot. *Phys. Rev. Lett.* **97**, 107401 (2006).
88. Manson, N. & Harrison, J. Photo-ionization of the nitrogen-vacancy center in diamond. *Diam. Relat. Mater.* **14**, 1705–1710 (2005).
89. Krebs, O., Benjamin, E. & Lemaitre, A. Magnetic anisotropy of singly Mn-doped InAs/GaAs quantum dots. *Phys. Rev. B* **80**, 165315 (2009).
90. Takahashi, S., Hanson, R., van Tol, J., Sherwin, M. S. & Awschalom, D. D. Quenching spin decoherence in diamond through spin bath polarization. *Phys. Rev. Lett.* **101**, 047601 (2008).
91. Averkiev, N., Gutkin, A., Kolchanova, N. & Reshchikov, M. Influence of uniaxial deformation on the Mn impurity photoluminescence band of GaAs. *Sov. Phys. Semicond.* **18**, 1019–1021 (1984).
92. Celebi, C. C. *et al.* Surface induced asymmetry of acceptor wave functions. *Phys. Rev. Lett.* **104**, 086404 (2010).
93. Jancu, J.-M. *et al.* STM images of subsurface Mn atoms in GaAs: Evidence of hybridization of surface and impurity states. *Phys. Rev. Lett.* **101**, 196801 (2008).
94. Bastard, G. Hydrogenic impurity states in a quantum well — a simple model. *Phys. Rev. B* **24**, 4714–4722 (1981).
95. Plot, B., Deveaud, B., Lambert, B., Chomette, A. & Regreny, A. Manganese luminescence in GaAs/GaAlAs superlattices. *J. Phys. C* **19**, 4279–4289 (1986).
96. Pereira, R. N. *et al.* Dielectric screening versus quantum confinement of phosphorus donors in silicon nanocrystals investigated by magnetic resonance. *Phys. Rev. B* **79**, 161304 (2009).
97. Pierre, M. *et al.* Single-donor ionization energies in a nanoscale CMOS channel. *Nature Nanotech.* **5**, 133–137 (2010).
98. Yakunin, A. M. *et al.* Spatial structure of Mn–Mn acceptor pairs in GaAs. *Phys. Rev. Lett.* **95**, 256402 (2005).
99. Childress, L. *et al.* Coherent dynamics of coupled electron and nuclear spin qubits in diamond. *Science* **314**, 281–285 (2006).
100. Epstein, R., Mendoza, F., Kato, Y. & Awschalom, D. Anisotropic interactions of a single spin and dark-spin spectroscopy in diamond. *Nature Phys.* **1**, 94–98 (2005).
101. Hanson, R., Dobrovitski, V., Feiguin, A., Gywat, O. & Awschalom, D. Coherent dynamics of a single spin interacting with an adjustable spin bath. *Science* **320**, 352–355 (2008).
102. Jiang, L. *et al.* Quantum repeater with encoding. *Phys. Rev. A* **79**, 032325 (2009).
103. Jelezko, F. *et al.* Observation of coherent oscillation of a single nuclear spin and realization of a two-qubit conditional quantum gate. *Phys. Rev. Lett.* **93**, 130501 (2004).
104. Neumann, P. *et al.* Multipartite entanglement among single spins in diamond. *Science* **320**, 1326–1329 (2008).
105. Hanson, R., Gywat, O. & Awschalom, D. D. Room-temperature manipulation and decoherence of a single spin in diamond. *Phys. Rev. B* **74**, 161203(R) (2006).
106. Taylor, J. M. *et al.* High-sensitivity diamond magnetometer with nanoscale resolution. *Nature Phys.* **4**, 810–816, (2008).
107. Degen, C. L. Scanning magnetic field microscope with a diamond single-spin sensor. *Appl. Phys. Lett.* **92**, 243111 (2008).
108. Maze, J. R. *et al.* Nanoscale magnetic sensing with an individual electronic spin in diamond. *Nature* **455**, 644–647 (2008).
109. Balasubramanian, G. *et al.* Nanoscale imaging magnetometry with diamond spins under ambient conditions. *Nature* **455**, 648–651 (2008).
110. Cole, J. H. & Hollenberg, L. C. L. Scanning quantum decoherence microscopy. *Nanotechnology* **20**, 495401 (2009).
111. Tan, K. Y. *et al.* Transport spectroscopy of single phosphorus donors in a silicon nanoscale transistor. *Nano Lett.* **10**, 11–15 (2010).
112. Hanson, R., Kouwenhoven, L. P., Petta, J. R., Tarucha, S. & Vandersypen, L. M. K. Spins in few-electron quantum dots. *Rev. Mod. Phys.* **79**, 1217 (2007).
113. Skolnick, M. & Mowbray, D. Self-assembled semiconductor quantum dots: Fundamental physics and device applications. *Annu. Rev. Mater. Res.* **34**, 181–218 (2007).
114. Strauf, S. *et al.* High-frequency single-photon source with polarization control. *Nature Photon.* **1**, 704–708 (2007).
115. Heiss, D., Jovanov, V., Bichler, M., Abstreiter, G. & Finley, J. J. Charge and spin readout scheme for single self-assembled quantum dots. *Phys. Rev. B* **77**, 235442 (2008).
116. Laucht, A. *et al.* Electrical control of spontaneous emission and strong coupling for a single quantum dot. *New J. Phys.* **11**, 023034 (2009).
117. Tyryshkin, A. M., Lyon, S. A., Astashkin, A. V. & Raitsimring, A. M. Electron spin relaxation times of phosphorus donors in silicon. *Phys. Rev. B* **68**, 193207 (2003).

Acknowledgements

We acknowledge valuable discussions with all participants at the workshop on Single Dopant Control, 29 March to 1 April 2010, at the Lorentz Center in Leiden. We also thank D. Awschalom, L. Besombes and S. Rogge for their suggestions and reading of the manuscript prior to submission. P.M.K. acknowledges support from VICI-Grant No. 6631, FOM, NAMASTE, SemiSpinNet and the Lorentz Center. M.E.F. acknowledges support from ARO, ONR and DARPA.